Absolute quantitation of iodine-123 epidepride kinetics using single-photon emission tomography: comparison with carbon-11 epidepride and positron emission tomography

Pedro Almeida[1,2], Maria João Ribeiro[1,3], Michel Bottlaender[1], Christian Loc'h[1], Oliver Langer[1], Daniel Strul[1], Patrick Hugonnard[4], Pierre Grangeat[4], Bernard Mazière[1], Bernard Bendriem[1]

[1] CEA, Service Hospitalier Frédéric Joliot, DSV/DRM, Orsay, France
[2] Hospital Garcia de Orta, Serviço de Medicina Nuclear, Bairro do Matadouro – Pragal, Almada, Portugal
[3] Serviço de Biofísica, IBILI, Faculdade de Medicina de Coimbra, Coimbra, Portugal
[4] CEA, Laboratoire d'Electronique de Technologie et d'Instrumentation, DTA/DSYS, Grenoble, France

Received 10 March and in revised form 14 June 1999

Abstract. Epidepride labelled with iodine-123 is a suitable probe for the in vivo imaging of striatal and extrastriatal dopamine D_2 receptors using single-photon emission tomography (SPET). Recently, this molecule has also been labelled with carbon-11. The goal of this work was to develop a method allowing the in vivo quantification of radioactivity uptake in baboon brain using SPET and to validate it using positron emission tomography (PET). SPET studies were performed in *Papio anubis* baboons using ^{123}I-epidepride. Emission and transmission measurements were acquired on a dual-headed system with variable head angulation and low-energy ultra-high resolution (LEUHR) collimation. The imaging protocol consisted of one transmission measurement (24 min, heads at 90°), obtained with two sliding line sources of gadolinium-153 prior to injection of 0.21–0.46 GBq of ^{123}I-epidepride, and 12 emission measurements starting 5 min post injection. For scatter correction (SC) we used a dual-window method adapted to ^{123}I. Collimator blurring correction (CBC) was done by deconvolution in Fourier space and attenuation correction (AT) was applied on a preliminary (CBC) filtered back-projection reconstruction using 12 iterations of a preconditioned, regularized minimal residual algorithm. For each reconstruction, a calibration factor was derived from a uniform cylinder filled with a ^{123}I solution of a known radioactivity concentration. Calibration and baboon images were systematically built with the same reconstruction parameters. Uncorrected (UNC) and (AT), (SC+AT) and (SC+CBC+AT) corrected images were compared. PET acquisitions using 0.11–0.44 GBq of ^{11}C-epidepride were performed on the same baboons and used as a reference. The radioactive concentrations expressed in percent of the injected dose per 100 ml (%ID/100 ml) obtained after (SC+CBC+AT) in SPET are in good agreement with those obtained with PET and ^{11}C-epidepride. A method for the in vivo absolute quantitation of ^{123}I-epidepride uptake using SPET has been developed which can be directly applied to other ^{123}I-labelled molecules used in the study of the dopamine system. Further work will consist in using PET to model the radioligand-receptor interactions and to derive a simplified model applicable in SPET.

Key words: Absolute quantitation – Single-photon emission tomography – Positron emission tomography – Dopamine receptors – Imaging

Eur J Nucl Med (1999) 26:1580–1588

Introduction

The human dopamine system is involved in the regulation of brain functions controlling motor, cognitive and motivational behaviours. Disruptions of its functioning have been implicated in neurological and psychiatric illnesses, as well as in some of the deficits associated with the aging of the human brain. In vivo imaging of dopamine receptors is therefore expected to contribute greatly to both the understanding of the human brain mechanisms and the treatment of psychiatric disorders.

During recent years, molecules with selective affinity for the dopamine D_2 receptors have been developed, labelled with short-lived isotopes and used to study receptor distribution in the living human brain by positron emission tomography (PET). PET imaging, however, requires a cyclotron and heavy hot chemistry facilities, which limit its application for clinical use.

Correspondence to: P. Almeida, Hospital Garcia de Orta, Serviço de Medicina Nuclear, Bairro do Matadouro – Pragal, P-2801 Almada, Portugal, e-mail: palmeida@correio.cc.fc.ul.pt, Tel.: +351-1-2940294, ext. 4080, Fax: +351-1-2957004

Given the widespread availability and lower costs of single-photon emission tomography (SPET) compared with PET, application of this technique for the imaging of the D_2 dopamine system may play an important clinical role. Several SPET radioligands have been developed for the study of dopamine receptors [1] and the investigation of Parkinson's disease [2]. Among these radioligands, the benzamide epidepride ((*S*)-5-iodo-*N*-((1-ethyl-2-pyrrolinidyl)methyl)-2,3-dimethoxybenzamide), a potent and highly selective dopamine D_2 receptor antagonist, has been labelled with iodine-123 [3]. The use of ^{123}I-epidepride has been reported in the imaging of pituitary adenoma [4], Parkinson's and Huntington's diseases and multiple system atrophy [5]. Its distribution and kinetics in human brain have recently been investigated [6].

Critical to the application of SPET for clinical studies of the dopamine receptors is the possibility of obtaining accurate quantitative information about radioactivity uptake. Using these measures to model the kinetics of the radioligand specific binding, the receptor density and relevant biochemical parameters could be obtained [7]. Such information could be used to help in patient follow-up and treatment monitoring. However, absolute quantitation of radioactive concentration is not possible before adequate compensation for scattered radiation, photon attenuation and collimator blurring effect, which are the main factors limiting the precision and accuracy of SPET imaging.

The effects of scatter and attenuation are recognized as important sources of bias in the quantitation of D_2 receptor binding obtained with SPET [8]. Scatter adds additional low-frequency blurr+ing to the projections and is responsible for reducing the contrast in reconstructed images. Scatter can be corrected using different approaches, such as methods based on multi-window acquisitions or adequate modelling in the image reconstruction algorithms [9].

Attenuation introduces large bias, generally leading to significant underestimation of radioactive concentration. Attenuation correction using a uniform ellipse encompassing the head has been shown not to be accurate enough in volumetric quantitation procedures if broad-beam attenuation coefficients are used [10–12]. Moreover, the non-homogeneity of the head itself may produce errors larger than 10% in activity quantitation if a uniform attenuation map is used. As a consequence it has been proposed that non-uniform attenuation correction is needed [12,13]. Attenuation can be corrected using patient-specific attenuation maps obtained in narrow-beam geometry using external line sources incorporated on gamma cameras [14,15], while improved spatial resolution can be obtained using either iterative approaches [16,17] or restoration filtering [18,19].

Recently, some molecules used in SPET have been labelled with positron emitters [20,21]. The use of the same molecule in PET and SPET allows direct comparison of the radioactive uptake measured with each technique. This approach therefore represents a suitable tool for the validation of quantitation methodologies developed for SPET if differences in labelled metabolites are accounted for during the comparison of results.

In this work, we present and evaluate a method to obtain absolute quantitation of radioactivity uptake in dopamine D_2-enriched structures of baboon brain in vivo, following the injection of ^{123}I-epidepride and SPET. In this method, scatter is compensated using a dual-window method adapted to ^{123}I while an iterative algorithm is used to correct for attenuation using transmission measurements. Collimator response is compensated by deconvolution in the Fourier space and, finally, the cross-calibration of the acquisition system is used to obtain values of the radioactive concentration in regions of interest. This quantification approach can be directly applied to study the uptake of other ^{123}I-labelled molecules targeting for the same cerebral structures. The results obtained are compared against PET measurements, using carbon-11 epidepride in the same animals, which were used as reference.

Materials and methods

Labelling of epidepride with ^{123}I and ^{11}C (Fig. 1)

^{123}I-epidepride was prepared according to the procedure described by Clanton et al. [22]. Briefly, radioiodinated epidepride was obtained by electrophilic substitution of a tributyltin leaving group by ^{123}I using chloramine-T as an oxidizing agent in the presence of diluted chlorhydric acid. The synthesis time was 2 min. The radiolabelled compound was purified by reverse-phase high-perfor-

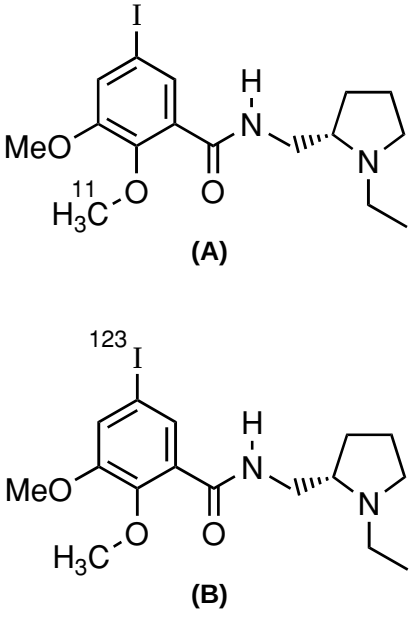

Fig. 1A, B. Chemical structure of epidepride: **A** labelled with ^{11}C for use in PET and **B** labelled with ^{123}I for use in SPET

mance liquid chromatography (HPLC) (μBondapak 7.8×300 mm, Waters) using a mixture of 0.01 *M* H_3PO_4/acetonitrile 80/20 V/V, flow rate 4 ml/min, and collected at 21 min. The chemical and radiochemical purities of ^{123}I-epidepride were higher than 99% and the specific radioactivity was greater than 1000 GBq/μmol.

^{11}C-epidepride was prepared by an O-alkylation reaction of the 2-hydroxy precursor with ^{11}C-methyl triflate in acetone, with sodium hydroxide as a base [20]. ^{11}C-epidepride was purified by normal phase on a Waters μ-Porasil column (7.8×300 mm, 10 μm) and a mixture of CH_2Cl_2/CH_3OH/Et_3N, 96/4/0.04, pH=8 as a mobile phase (flow rate 2 ml/min). The total synthesis time was 30 min and the specific radioactivity 14–18 GBq/μmol.

Baboons

All animal procedures used were in strict compliance with the European Union legislation for the Care and Use of Laboratory Animals (86/609-EEC). Experiments were carried out on two male *Papio anubis* baboons weighing approximately 15 kg each. Baboon 1 was studied once with both SPET and PET while baboon 2 was imaged twice using SPET (test and re-test experiments) and only once using PET.

Two days before emission studies, the potential uptake of free ^{123}I in thyroid was blocked by oral administration of Lugol. Before PET and SPET studies, all animals received 15 mg/kg of ketamine and were intubated. During experiments anaesthesia was maintained by ventilation using 1% isoflurane.

During the whole acquisition process, the baboon's head was fixed to the system bed using a head-holder to ensure reproducible positioning between scans. In both PET and SPET studies, radioligands were injected intravenously (i.v.) as a 30-s bolus.

SPET

Imaging. Emission and transmission data were collected on a dual-headed DST gamma camera (SMV, Buc, France) equipped with parallel, low-energy ultra-high resolution (LEUHR) collimators. Transmission measurement was achieved with two collimated scanning line sources of gadolinium-153 (100 keV) with a total activity of 2.8 GBq and performed in a 90–110 keV window. Transmitted photons were collected in a 3-cm-wide electronic spatial window synchronized with the sources' motion. Such electronic windowing defines two different regions for the detection of transmitted and emitted events. Sixty-four views were acquired over a 180° orbit with detection heads at 90°.

After transmission scans, emission data were measured with detection heads at 180° over a 360° orbit, in two energy windows. One, defined as 146–175 keV, collected primary photons while the other, placed at 90–110 keV, was used for the estimation of scatter. The total count rate during emission studies was always inferior to 14 kcts/s, avoiding dead-time effects which only become significant above 20 kcts/s.

Both transmission and emission acquisitions used 128×128 pixel matrices, resulting in square pixels with 3.4×3.4 mm. The change in acquisition orbit allowed a good angular sampling in emission scans and avoided object deformation that may result from 180° imaging. To accommodate the use of a head support, the radius of rotation for both transmission and emission studies was 24 cm.

After the collection of a reference scan with the collimated line sources, the acquisition protocol consisted of the measurement of transmission projections for 45 s per view (28 min total acquisition time). The transmission measurements were followed by emission scans using 459 MBq (~0.1 nmol), 315 MBq (~1.0 nmol) and 211 MBq (26 nmol) of ^{123}I-epidepride i.v. injected in baboon 1, and in baboon 2 during the test and re-test experiments respectively. For each baboon, 12 consecutive tomographic studies were performed, each using 10 s per view, for a total scanning time of 18 min. The acquisition time for the whole protocol was approximately 4 h, with 2 min between each study. Due to the low sensitivity of SPET and the rapid accumulation of ^{123}I-epidepride in striatal regions, emission acquisitions started 5 min post-injection (p.i.).

Image reconstruction. Attenuation maps were reconstructed by filtered back-projection of the logarithm of the ratio between the reference and the transmission projections, with a Hanning apodisation window (0.5 cycles/pixel). The attenuation coefficients obtained were scaled to the ^{123}I energy. Before image reconstruction, scatter correction (SC) was performed on emission projections using a dual-window method experimentally adapted to ^{123}I (the method is described in detail in the Appendix).

The effects of collimator blurring on spatial resolution were modelled as a linear function of the source-collimator distance. An inverse Fourier deconvolution filter was used for collimator blurring compensation (CBC) [19].

Attenuation correction was performed on images as acquired (AT) or after scatter correction (SC+AT) or after scatter correction and collimator blurring compensation (SC+CBC+AT), using 12 iterations of a preconditioned, regularized, iterative, least-squares minimal residual algorithm and Hanning apodisation (0.5 cycles/pixel) [23]. Uncorrected (UNC) images were obtained for comparison. Processing times on a SUN SPARK 30 unit (Sun Microsystems) were approximately 25 and 10 min for (SC+CBC+AT) and (SC+AT) respectively. Reconstructed emission volumes consisted of 64 slices with a voxel of 3.4×3.4×6.8 mm and were corrected for ^{123}I decay.

Cross-calibration

Calibration of emission studies was obtained with a uniform cylinder (14.8 cm in diameter and 5 cm long) filled with a uniform ^{123}I solution. The radioactive concentration of this solution was assessed in a well-counter, yielding a value of 40 kBq/ml. Emission and transmission scans were obtained using the protocol just described and a large region of interest (ROI) was placed on a central slice of the reconstructed volume. Dividing the mean counts per pixel calculated in this ROI by the radioactivity concentration yielded the system sensitivity for each reconstruction.

PET

PET experiments were conducted in 2D mode on an ECAT 953B/31 system (Siemens/CTI, Knoxville, Tenn., USA), a brain-dedicated scanner allowing the simultaneous acquisition of 31 slices. The detailed technical and physical characteristics of this scanner are described elsewhere [24].

Acquisitions started prior to radioligand injection with a 15-min transmission scan, using three rod sources of germanium-68 (260 MBq). Emission studies consisted of a dynamic series of 34 scans. These scans started at the i.v. injection of 111 MBq (8.6 nmol) and 436 MBq (30 nmol) of ^{11}C-epidepride for baboon 1 and baboon 2 respectively. Data collection lasted for 123 min, fol-

Table 1. Experimental protocol used in PET imaging

Number of scans	Duration of each scan (min)	Total time (min)
5	1	5
5	3.6	*23*
1	2	25
5	3.6	*43*
1	2	45
3	6	*63*
1	2	65
3	6	*83*
1	2	85
5	3.6	*103*
1	2	105
3	6	*123*

The values in *italics* correspond to experimental points used to compare PET and SPET images

lowing an imaging protocol designed to match the time schedule used in SPET and described in Table 1. The detection of scattered photons was minimized by the use of interplane septa and was neglected. Image reconstruction was done by filtered back-projection and Hanning apodisation (0.5 cycles/cm), resulting in reconstructed volumes with a 1.96×1.96×3.38 mm voxel size. All emission images were corrected for detector dead-time effects and ^{11}C decay.

ROI definition

For each baboon, a magnetic resonance imaging (MRI) acquisition was performed on a 1.5-T SIGNA scanner (General Electric Medical Systems, Milwaukee, Wis., USA). MRI and SPET images were resampled to PET voxel size. MRI resampling used software developed in our laboratory while in SPET, a cubic spline interpolation algorithm was applied. In both cases, conservation of mean counts per pixel was verified. Anatomical ROIs were then defined on MRI images, in regions corresponding to the striata and the cerebellum, and applied on PET and SPET slices obtained after image registration [25].

Validation of SPET results

SPET results were compared with PET measurements, which were used as references. PET scans were organized to match the time sampling obtained in SPET. Uptake values, measured as the percentage of the injected dose per 100 ml of tissue (%ID/100 ml), were used for the comparison. Values of percent normalized errors $Err(t)(\%)$, were calculated as a function of time using the expression:

$$Err(t)(\%) = \frac{|PET(t) - SPET(t)|}{PET(t)} \cdot 100, \quad (1)$$

where $PET(t)$ and $SPET(t)$ are the values of %ID/100 ml obtained at time t.

Two separate SPET acquisitions were performed on the same baboon and used to estimate the variability of SPET measurement. From these data, an index $\Delta S(t)$ (%) was derived as:

$$\Delta S(t)(\%) = \frac{|SPET_t(t) - SPET_n(t)|}{SPET_t(t)} \cdot 100, \quad (2)$$

where $SPET_t(t)$ and $SPET_{rt}(t)$ are the values obtained at time t for the first (test) and the second (re-test) experiments respectively.

From Eq. 1 and Eq. 2, mean values of $Err(\%)$ and $\Delta S(\%)$ were obtained as a function of reconstruction scheme by averaging the values obtained at each acquisition time.

The comparison of PET and SPET results was based on experiments performed on the same animal to guarantee similar biological conditions.

Evaluation of partial volume effects

PET and SPET acquisitions were performed to evaluate activity recovery using a resolution phantom (Jaszczak Deluxe phantom, DataSpectrum Corporation, Hillsborough, N.C., USA). The six spheres of the phantom (with diameters of 33.6, 27.8, 22.1, 15.5, 13.2 and 10.4 mm) were filled with a uniform radioactive solution of ^{123}I (SPET) or a uniform radioactive solution of ^{11}C (PET) and positioned in a cylinder filled with water.

PET consisted of a static acquisition of 2 min. In SPET, the acquisition protocol described previously, with 30 s per projection for emission studies, was used. After image reconstruction of PET scans, 9-pixel ROIs were used to measure the values of activity concentration at the centre of each sphere. These values were divided by the activity concentration in the largest sphere [for SPET taken on the (SC+CBC+AT) image] to obtain activity recovery coefficients (RCs) as a function of structure size.

Results

Attenuation maps

Examples of attenuation maps obtained in SPET are shown in Fig. 2. The vertical bars represent the headholder used in experiments.

The values of attenuation coefficients obtained after reconstruction and scaling to emission energy were measured on regions corresponding to brain tissue and bone using hand-drawn ROIs. The values obtained were 0.16±0.01 cm^{-1} for brain tissue and 0.23±0.03 cm^{-1} for bone.

Radioactivity uptake

In Fig. 3, the values of %ID/100 ml for ^{11}C-epidepride in baboon 1 measured by PET are shown. The uptake values in the striata showed a rapid increase at early times up to about 25 min p.i. and a continuous slow increase thereafter. In the cerebellum, the relatively high uptakes at early times decreased rapidly with time (approximately 15% of the initial radioactivity was present at 85 min p.i.).

Figure 4 shows typical emission maps obtained with the different SPET reconstruction protocols at 65 min p.i. Visual comparison of these images demonstrates the

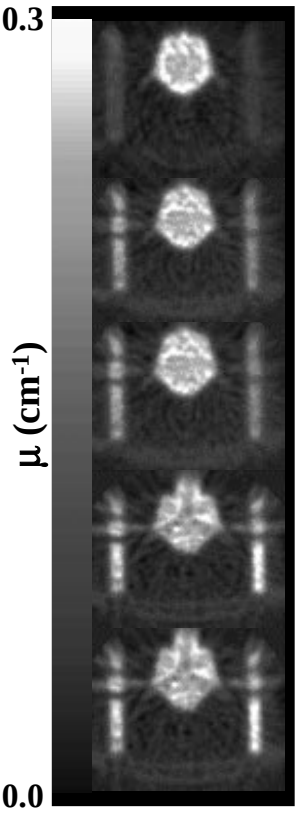

Fig. 2. Attenuation map of baboon's brain at several axial positions

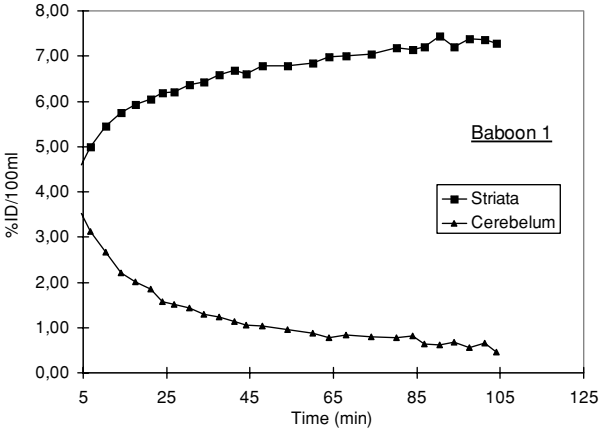

Fig. 3. Example of ^{11}C-epidepride kinetics used as reference. Results are expressed in percent of injected dose per 100 ml (%ID/100 ml)

improvement obtained using (CBC) SPET when compared with the PET reference image.

In Table 2, the kinetics obtained for baboon 1 by SPET after applying the different types of image correction is compared with those obtained by PET. The corresponding values are shown together with the respective values of *Err*(*%*) (Eq. 1). For the striata, *Err*(*%*) mean values decreased from 53% for uncorrected SPET images to 3% after (SC+CBC+AT) corrections. For the cerebellum, the differences from PET were significant for (SC+AT) and (SC+CBC+AT) SPET only after 85 min p.i.

The kinetics obtained for baboon 2 are shown in Table 3, where the test and re-test (SC+CBC+AT) SPET results are compared with those measured by PET. The values obtained for this comparison as well as the respective values of *Err*(*%*) (Eq. 1) and ΔS(*%*) (Eq. 2) are

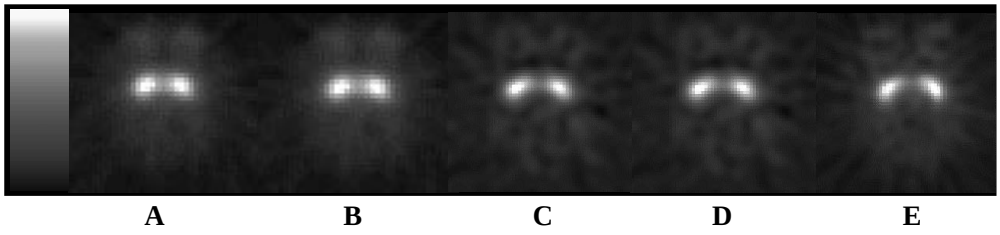

Fig. 4A–E. Emission maps at 65 min. p.i. **A** (UNC) SPET; **B** (AT) SPET; **C** (SC+AT) SPET; **D** (SC+CBC+AT) SPET; **E** PET

Table 2. Comparison of SPET and PET values of %ID/100 ml in striata (STR) and cerebellum (CRB) for baboon 1

Region	Correction	Time p.i. (min)			
		45	65	85	105
STR	UNC	3.30 (52)	3.37 (52)	3.37 (54)	3.38 (54)
	AT	5.09 (25)	5.21 (26)	5.20 (29)	5.23 (29)
	SC+AT	5.78 (15)	5.94 (16)	5.95 (19)	5.99 (19)
	SC+CBC+AT	7.06 (4)	7.33 (4)	7.49 (2)	7.55 (2)
	PET	6.81	7.07	7.32	7.37
CRB	UNC	0.62 (35)	0.51 (36)	0.42 (33)	0.37 (39)
	AT	1.32 (39)	1.10 (38)	0.88 (40)	0.79 (30)
	SC+AT	1.20 (26)	0.96 (20)	0.72 (14)	0.63 (3)
	SC+CBC+AT	1.31 (38)	1.07 (34)	0.74 (17)	0.65 (7)
	PET	0.95	0.80	0.63	0.61

Err(*%*) values (Eq. 1 in text) are shown in parentheses. Injected masses were respectively <0.1 nmol (SPET) and 8.6 nmol (PET)

Table 3. Values of %ID/100 ml obtained for experiments using baboon 2 in SPET (*t*, test; *rt*, re-test) and PET. *Err*(%) values (Eq. 1 in text) and $\Delta S(\%)$ values (Eq. 2 in text) are also shown. Injected masses were 1 nmol (test), 26 nmol (re-test) and 30 nmol (PET) respectively

Region	Correction	Time p.i. (min)											
		45			65			85			105		
		t/rt	$\Delta S(\%)$	*Err*(%)	*t/rt*	$\Delta S(\%)$	*Err*(%)	*t/rt*	$\Delta S(\%)$	*Err*(%)	t\rt	?S(%)	*Err*(%)
STR	UNC	1.10/1.00	9	51	1.17/1.06	9	53	1.19/1.10	8	54	1.22\1.13	7	54
	AT	1.86/1.67	10	19	1.89/1.77	6	24	1.91/1.83	4	26	1.96\1.88	4	25
	SC+AT	1.97/1.75	11	14	2.01/1.82	9	19	2.14/1.87	13	17	2.13\2.00	13	19
	SC+CBC+AT	2.16/2.15	0.4	6	2.25/2.26	0.4	10	2.39/2.36	1	7	2.43\2.54	1	8
	PET	2.29			2.49			2.58			2.63		
CRB	UNC	0.33/0.26	21	28	0.27/0.18	33	31	0.20/0.15	25	31	0.18\0.11	39	31
	AT	0.67/0.58	13	46	0.55/0.41	25	41	0.41/0.39	5	41	0.39\0.28	28	50
	SC+AT	0.54/0.54	0	18	0.41/0.29	29	5	0.35/0.32	9	20	0.29\0.22	24	12
	SC+CBC+AT	0.57/0.59	3	24	0.42/0.24	43	8	0.35/0.31	11	20	0.30\0.20	33	15
	PET	0.46			0.39			0.29			0.26		

Table 4. Comparative table of RC values obtained in PET and in SPET, using the Jaszczak resolution phantom. These values were used to assess the activity recovery on small hot structures

Sphere diameter (mm)	RC values			
	SPET (AT)	SPET (SC+AT)	SPET (SC+CBC+AT)	PET
33.6	0.69	0.99	1.00	1.00
27.7	0.59	0.87	0.99	0.99
22.4	0.45	0.68	0.85	0.97
15.2	0.21	0.32	0.48	0.80
13.6	0.13	0.19	0.33	0.67
10.4	0.07	0.09	0.15	0.45

also shown. The SPET/PET comparison presented in Table 3 shows good agreement between the two measurements. For the striata, the *Err*(%) mean values decreased from 53% for uncorrected SPET images to 8% after (SC+CBC+AT) corrections. In the cerebellum, the mean *Err*(%) was about 15% after corrections compared with 30% before them. Moreover, joint analysis of Tables 2 and 3 shows that for this region, applying only attenuation correction may produce less accurate results than are obtained with uncorrected images.

For the striata, the mean $\Delta S(\%)$ values (Eq. 2) were 8%, 6%, 12% and 1% for (UNC), (AT), (SC+AT) and (SC+CBC+AT) respectively. For the cerebellum, the mean values of $\Delta S(\%)$ were 30%, 18%, 16% and 23% for (UNC), (AT), (SC+AT) and (SC+CBC+AT) images respectively. These values are much larger than those measured for the striata, probably because this structure is more affected by statistical fluctuations (lower radioactivity uptake). Finally, it should be noted that attenuation correction leads to approximately a twofold increase in measured radioactivity for both the striata and the cerebellum and that striatal uptake is also affected by spatial resolution.

Evaluation of partial volume effects

Figure 5 shows examples of transaxial slices obtained at the sphere equators for SPET (SC+AT and SC+CBC+AT) and PET. Partial volume effects result in an underestimation of the radioactivity concentration, which is visible for the smaller structures.

The RC values obtained in SPET and PET are shown in Table 4. The effects of applying different sets of corrections on SPET images are demonstrated therein. For structures with a size close to that of baboon striata (~22 mm in diameter), RC values show that SPET can recover 0.45 (AT) or 0.68 (SC+AT) of the injected radioactivity. If CBC is also applied, this value increases to 0.85. For the same sphere, RC measured with PET is 0.97.

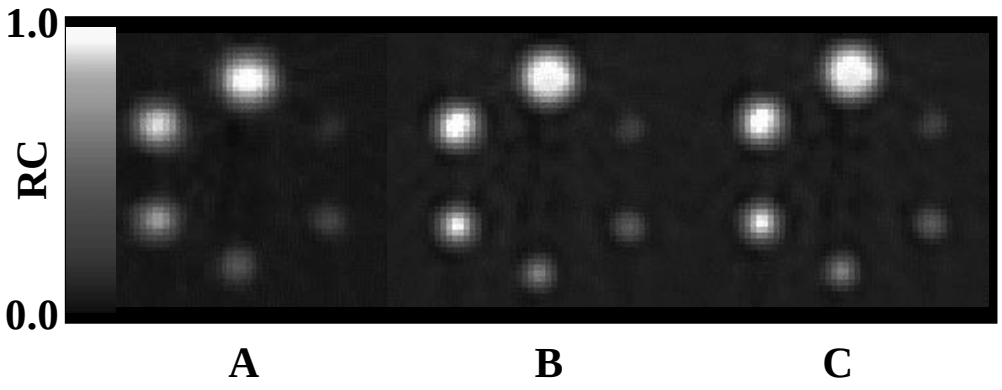

Fig. 5A–C. Transaxial slices obtained for the Jaszczak phantom used in the evaluation of RC values. **A** (SC+AT) SPET; **B** (SC+CBC+AT) SPET; **C** PET

Discussion

In this study, we have presented a method to quantify the radioactivity concentrations measured by SPET in vivo. The method includes corrections for the main effects degrading the accuracy and precision of SPET and is intended to produce absolute quantitation of radioactivity. Since absolute quantitation is routinely obtained in PET, PET acquisitions were also been performed and used as references. For this purpose, the same radioligand was isotopically labelled with appropriate single-photon or positron emitter isotopes. SPET and PET studies were then performed on the same baboons and analysed using the same anatomical ROIs. Baboon 1 presented a much higher uptake of ^{123}I-epidepride (approximately threefold) than baboon 2. The same inter-individual variation was observed in PET and in SPET and may therefore be biological.

The results obtained show that attenuation is a very penalizing effect in the studies of brain structures. Attenuation correction alone is responsible for approximately a twofold increase in the radioactivity uptake values. The accuracy of SPET quantitative measurement in the striata improves with the successive application of image corrections. Quantitation is clearly inaccurate if no image correction is applied. If only attenuation is applied, the remaining differences compared with PET exceed 24%. Additional scatter correction reduces these differences to 17%. This reinforces the importance of scatter correction in quantitative measurements of brain radioactivity uptake. However, accurate measurements are only achieved after (CBC) correction, although differences between PET and (SC+CBC+AT) SPET were generally smaller than those expected from differences in partial volume effects alone.

In the cerebellum, SPET results suffer from high statistical uncertainty due to the low radioactivity uptake of a radioligand with such a high selectivity for D_2 dopamine receptors. The mean differences observed between SPET with (SC+CBC+AT) and PET were less than 24% and the measured values with SPET were generally higher than those measured using PET. Note that for the cerebellum the (CBC) correction does not lead to a major change in measured values when compared with those obtained after (SC+AT) corrections only. This is an expected result for a large structure like the cerebellum. The observed overestimation could result from a suboptimal scatter correction.

Practical issues dictated the choice of the scatter correction method. A dual-window method was used as our SPET system does not allow collection of more than two energy windows in tomographic mode. The scatter window was chosen in order to allow the potential use of simultaneous emission and transmission measurements in a simple way. In fact, during simultaneous imaging the system provides a 90–110 keV data set collected in the outer part of the electronic window, which could be used for scatter correction. However, it is known that correction for scatter by subtracting from the conventional window a fraction k of the image corresponding to events detected in a secondary energy window is not theoretically correct and that scatter depends on the particular radioactivity and tissue density distribution. Moreover, the energy difference between the scatter window used and the ^{123}I window was high, and thus photons that had scattered at large angles were collected in that window. Therefore, the subtraction of these photons would not have been spatially adapted to the scatter distribution within the photopeak window and might have resulted in second-order errors. In addition, we used two cold regions inside a hot phantom to estimate the factor k although the imaging conditions relate to hot structures in a cold background. Moreover, regions of high attenuation coefficient located near the cerebellum (such as bone) that can produce significant amounts of scatter were not taken into account. These factors can explain the general overestimation of SPET compared with PET in the cerebellum and in the striata if differences in partial volume effects between the two techniques are taken into account. The strategy for scatter correction must therefore be refined or substituted. The use of hot structures inside a colder phantom and the use of a scatter window closer to the photopeak energy would probably allow better scatter estimation.

In SPET, the loss in spatial resolution was compensated using the described (CBC) correction. Such correction

usually results in a slight increase in the measured values of radioactivity concentration even at the cerebellum and in the fluctuations visible in the re-test experiment. These effects are probably due to noise amplification resulting from the deconvolution process. This noise amplification adds to that generated by the scatter subtraction method used in the present approach. Further efforts must therefore be made to optimize regularization parameters in order to control these effects. On the other hand, the methodology described is simple and can be used on any nuclear medicine equipment using a transmission measurement system and adequate reconstruction software for attenuation and (CBC) compensation.

The comparison of test and re-test acquisitions allowed us to obtain a first estimate of the reproducibility of quantitative measurement of ^{123}I-epidepride in SPET. The mean relative normalized differences found between the two studies for (SC+CBC+AT) images were 1% (striata) and 23% (cerebellum) for the time points presented in Table 3. Seibyl et al. [26] have reported mean intrasubject variability of 12.8% in the striata and 16.5% in the occipital cortex using ^{123}I-β-CIT in humans.

The use of two labelling strategies, one using a positron emitter and the other a single-photon emitter on the same molecule, is a powerful tool with which to validate SPET quantification. Such a method is, of course, applicable to ^{123}I, or with minor modifications to technetium-99m and to various radioligands developed for the imaging of brain, heart or other organs, e.g. TRODAT-1 [27].

Some precautions must be taken concerning the different active metabolites associated with a given ligand labelled with different radioisotopes. In the context of the study reported here, comparing results obtained using ^{123}I-epidepride in SPET and ^{124}I-epidepride in PET could have minimized this problem. However, during this study we did not have access to ^{124}I. Metabolite studies of ^{123}I-epidepride and ^{11}C-epidepride in *Papio anubis* baboons performed by HPLC according to a standardized method [28] demonstrated that the radio-HPLC profiles of ^{123}I-epidepride and of ^{11}C-epidepride were identical and showed two main radioactive peaks. One of these peaks was a polar hydrophilic peak coming in the solvent front, and the other was the unchanged radiolabelled ligand. Only small differences in minor radioactive peaks were observed. The polar metabolite is not likely to cross the blood-brain barrier. The kinetics of the unchanged portion of the two radiolabelled ligands in plasma was similar. Therefore, we do not anticipate differences between PET and SPET data resulting from different metabolic pathways.

Future work will consist in using PET measurements of the radioligand kinetics to model the radioligand-receptor interaction for ^{11}C-epidepride and in deriving a simplified model applicable to SPET.

In conclusion: We have developed a methodology to quantify the radioactive uptake in dopamine D_2 receptor radioligand studies in vivo using SPET. The results obtained using ^{123}I-epidepride, after appropriate system calibration and image corrections, were compared with the results of PET acquisitions using ^{11}C-epidepride in the same baboons. Despite the presence of some limitations, which were discussed, the application of the proposed methodology significantly reduces the differences observed between PET and uncorrected SPET images and validates the accuracy of absolute quantitation of radioactivity using SPET. The method can be directly applied to other ^{123}I-labelled radioligands and, with minor modifications, to ^{99m}Tc-labelled molecules.

Acknowledgements. The authors thank Régine Trebossen for helpful discussions on the comparison of PET and SPET results and C. Fuseau, O. Lamer, V. Brulon and P. Merceron for technical assistance during PET and SPET experiments. They are also indebted to the cyclotron staff for providing ^{11}C and to F. Dollé for assisting in the preparation of ^{11}C-epidepride. This work was partially supported by the BIOMED II Program CPFIDOTS and by the Medical Imaging Research Program of the CNRS (France). P.A. and M.J.R. were partially supported by Fundação para a Ciência e Tecnologia (Portugal) (Ph.D. grants PRAXIS-XXI/BD/3300/94 and PRAXIS-XXI/BD/2657/94). M.J.R. was also supported by A.R.S. (Portugal). O.L. was supported by a grant from "Human Capital and Mobility" from the EEC, contract number ERBCHBGTC940716.

Appendix: Adaptation of the dual-window scatter correction method to ^{123}I

Scatter correction (SC) used the dual-energy window method proposed by Jaszczak [29]. It was adapted to the energy of ^{123}I photons and to the acquisition windows applied using the following procedure: A cylindrical phantom with two fillable cylindrical inserts [30] was used to derive the proportionality factor *k* used for scatter correction. Its cylindrical part was filled with a ^{123}I uniform solution of 17 kBq/ml and the two inserts filled with water. Photopeak and scatter data were acquired using 30 s per projection and were then combined using values of *k* ranging from 0.0 to 1.2. The resulting projections were reconstructed by filtered back-projection us-

Table A1. Evolution of mean counts per pixel in "cold" cylinders as a function of *k*. The result of fitting this variation by a linear function is shown in the bottom row. The *k* value used was obtained after solving it to zero

Value of *k*	Mean value of counts per pixel
0	198
0.5	106
0.8	44
1	10.5
1.1	–5.2
1.2	–21.5
Mean counts per pixel = –184.74 *k*+196.93	

ing a Hanning window (0.5 cycles/cm cut-off). A slice was visually selected on the reconstructed volume and circular regions of interest were placed on each of the two "cold" cylinders. The measured values of mean count per pixel were plotted as a linear function of k, which was then solved to zero, to yield an optimum k value of k=1.06. The dependence of counts per pixel in the "cold" regions on k and resulting function are shown in Table A1.

References

1. Iwasaki Y, Yonekura Y, Saji H, et al. SPECT imaging of dopamine D2 receptors with 2'-iodospiperone. *J Nucl Med* 1996; 36**:** 1191–1195.
2. Asenbaum S, Brucke T, Pirker W, et al. Imaging of dopamine transporters with iodine-123-beta-CIT and SPECT in Parkinson's disease. *J Nucl Med* 1997; 38**:** 1–6.
3. Kessler RM, Mason NS, Votaw JR, et al. Visualization of extrastriatal dopamine D2 receptors in the human brain. *Eur J Pharmacol* 1992; 223**:** 105–107.
4. Pirker W, Riedl M, Luger A, et al. Dopamine D2 receptor imaging in pituitary adenomas using iodine-123-epidepride and SPECT. *J Nucl Med* 1996; 37**:** 1931–1937.
5. Pirker W, Asenbaum S, Wenger S, et al. Iodine-123-epidepride-SPECT: studies in Parkinson's disease, multiple system atrophy and Huntington's disease. *J Nucl Med* 1997; 38**:** 1711–1717.
6. Kuikka JT, Akerman KK, Hiltunen J, et al. Striatal and extrastriatal imaging of dopamine D_2 receptors in the living human brain with ^{123}I-epidepride single-photon emission tomography. *Eur J Nucl Med* 1997; 24**:** 483–487.
7. Delforge J, Loc'h C, Hantraye P, et al. Kinetic analysis of central ^{76}Br-bromolisuride binding to dopamine D2 receptors studied by PET. *J Cereb Blood Flow Metab* 1991; 11**:** 914–925.
8. Hashimoto J, Takatoku K, Bando K, et al. Effects of scatter and attenuation correction on quantitative analysis of beta-CIT brain SPECT [abstract]. *J Nucl Med* 1997; 38(Suppl)**:** 146P.
9. Buvat I, Benali H, Todd-Pokropek A, Di Paola R. Scatter correction in scintigraphy: the state of the art. *Eur J Nucl Med* 1994; 21**:** 675–694.
10. Kemp BJ, Prato FS, Dean GW, Nicholson RL, Reese L. Correction for attenuation in technetium-99m-HMPAO SPECT brain imaging. *J Nucl Med* 1992; 33**:** 1875–1880.
11. Kemp BJ, Prato FS, Nicholson RL, Reese L. Transmission computed tomography imaging of the head with a SPECT system and a collimated line source. *J Nucl Med* 1995; 36**:** 328–335.
12. Stodilka RZ, Kemp BJ, Prato FS, Nicholson RL. Importance of bone attenuation in brain SPECT quantification. *J Nucl Med* 1998; 39**:** 190–197.
13. Glick SJ, King MA, Pan T-S, Soares EJ. Compensation for nonuniform attenuation in SPECT brain imaging. *IEEE Trans Nucl Sci* 1996; 43**:** 737–750.
14. Tan P, Bailey DL, Meikle SR, Eberl S, Fulton RR, Hutton BF. A scanning line source for simultaneous emission and transmission measurements in SPECT. *J Nucl Med* 1993; 34**:** 1752–1760.
15. Bailey DL. Transmission scanning in emission tomography. *Eur J Nucl Med* 1998; 25**:** 774–787.
16. Passeri A, Formiconi AR, Meldolesi U. Physical modeling (geometrical system response, Compton scattering and attenuation) in brain SPECT using the conjugate gradients reconstruction method. *Phys Med Biol* 1992; 37**:** 1727–1744.
17. Riddell C, Bendriem B, Bourguignon MH, Kernevez J-P. The approximate inverse and conjugate gradient: non-symmetrical algorithms for fast attenuation correction in SPECT. *Phys Med Biol* 1995; 40**:** 269–281.
18. Pretorius PH, King MA, Glick SJ, Pan T-S, Luo D-S. Reducing the effect of nonstationary resolution on activity quantitation with the frequency distance relationship in SPECT. *IEEE Trans Nucl Sci* 1996; 43**:** 3335–3341.
19. Sire P, Grangeat S, Iovleff S, La V, Mallon A. *Proceedings of the IEEE Nuclear Science and Medical Imaging Conference*, vol. 3. Anaheim, California (USA) 1996, pp 1633–1637.
20. Langer O, Halldin C, Dolle F, et al. Carbon-11 epidepride: a suitable radioligand for PET investigation of striatal and extrastriatal dopamine D2 receptors. *Nucl Med Biol*, 1999; in press.
21. Westera G, Buck A, Burger C, Leenders KL, von Schulthess GK, Schubinger AP. Carbon-11 and iodine-123 labeled iomazenil: a direct PET-SPET comparison. *Eur J Nucl Med* 1996; 23**:** 5–12.
22. Clanton, JA, de Paulis T, Schmidt DE, et al. Preparation of [123I]epidepride: a dopamine D-2 receptor antagonist radioligand. *J Label Comp Radiopharm* 1991; XXIX**:** 745–751.
23. La V, Grangeat P. Minimal residual cone-beam reconstruction with attenuation correction in SPECT. *Phys Med Biol* 1998; 43**:** 715–727.
24. Spinks TJ, Jones T, Bailey DL, et al. Physical performance of a positron tomograph for brain imaging with retractable septa. *Phys Med Biol* 1992; 37**:** 1637–1655.
25. Mangin J-F, Frouin V, Bloch I, Bendriem B, Lopez-Krahe J. Fast nonsupervised 3D registration of PET and MR images of the brain. *J Cereb Blood Flow Metab* 1994; 14**:** 749–762.
26. Seibyl JP, Laruelle M, van Dick CH, et al. Reproducibility of iodine-123-beta-CIT SPECT brain measurement of dopamine transporters. *J Nucl Med* 1996; 37**:** 222–228.
27. Kung M-P, Stevenson DA, Plossl K, et al. ^{99m}Tc-TRODAT-1: a novel technetium-99m complex as a dopamine transporter imaging agent. *Eur J Nucl Med* 1997; 24**:** 372–380.
28. Bergström KA, Halldin C, Yu MX, et al. The metabolite pattern of [^{123}I]epidepride in human plasma determined with a gradient HPLC method. *J Label Comp Radiopharm* 1997; XL**:** 151–153.
29. Jaszczak RJ, Greer KL, Floyd CE Jr, Harris CC, Colleman ER. Improved SPECT quantification using compensation for scattered photons. *J Nucl Med* 1984; 25**:** 893–900.
30. Townsend DW, Choi Y, Sashin D, Mintun M. An investigation of practical scatter correction techniques for 3D PET [abstract]. *J Nucl Med* 1994; 35(Suppl)**:** 50P.